MOIRCS: Multi-object Infrared Camera and Spectrograph for SUBARU

Takashi Ichikawa[a], Ryuji Suzuki[a,b], Chihiro Tokoku[a,b], Yuka Katsuno Uchimoto[a,b,c], Masahiro Konishi[a,b], Tomohiro Yoshikawa[a,b], Toru Yamada[b,d], Ichi Tanaka[a,b], Koji Omata[b], and Tetsuo Nishimura[b]

[a]Astronomical Institute, Tohoku University, Aoba, Sendai 980-8578, Japan;
[b]Subaru Telescope, 650 North A'ohoku Place, Hilo, Hawaii 96720;
[c]Institute of Astronomy, University of Tokyo, 2-21-1 Osawa, Mitaka 181-0015, Japan;
[d]National Astronomical Observatory of Japan, 2-21-1 Osawa, Mitaka 181-8588, Japan

ABSTRACT

MOIRCS is a new Cassegrain instrument of Subaru telescope, dedicated specifically for wide field imaging and multi-object spectroscopy in near-infrared. MOIRCS has been constructed jointly by Tohoku University and the Subaru Telescope and saw the first light in Sep, 2004. The commissioning observations to study both imaging and spectroscopic performance were conducted for about one year. MOIRCS mounts two 2048×2048 HAWAII2 arrays and provides a field of view of $4' \times 7'$ with a pixel scale of $0''.117$. All-lens optical design is optimized for 0.8 to 2.5 μm with no practical chromatic aberration. Observations confirm the high image quality over the field of view without any perceptible degradation even at the field edge. The best seeing we have obtained so far is FWHM$= 0''.18$. A novel design of MOIRCS enables us to perform multi-object spectroscopy with aluminum slit masks, which are housed in a carrousel dewar and cooled to ~ 110 K. When choosing MOS mode, a manipulator pulls out a slit mask from the carrousel into the MOIRCS main dewar and sets it properly at the Cassegrain focus. The carrousel is shuttered by a gate valve, so that it can be warmed and cooled independently to exchange slit-mask sets during daytime. We have tested various configurations of 30 or more multi-slit positions in various sky fields and found that targets are dropped at the centers of slits or guide holes within a dispersion of about 0.3 pixels ($0''.03$). MOIRCS has been open to common use specifically for imaging observations since Feb. 2006. The MOS function will be available in next August.

Keywords: Near-infrared, imaging, wide field, multi objects, spectrograph, Subaru

1. INTRODUCTION

With the recent advent of large format near-infrared focal plane arrays (FPAs), astronomers will explore deeper and even wider space into the universe in near-infrared bands. For example, the study of formation and evolution of galaxies at the high-z universe, which is one of the central issues in modern astronomy, has been greatly progressed by the wide field imaging in near-infrared. Since the optical wavelengths correspond to UV region in rest frame at $z > 1$, observations in optical generally show the temporal star forming activity in galaxies. The near-infrared, on the other hand, depicts the feature of galaxies at optical in rest frame for such high-z galaxies.

Although the powerful near-infrared instruments, such as ISSAC[1] at VLT in the southern hemisphere and CISCO[2] in the northern hemisphere, have elucidated the nature of star formation history and galaxy evolution at the high-z universe, the field of view is not large enough to study the general nature of galaxy evolution due to the cosmic variance. The small field of view would not be competent to study large scale clustering of galaxies. Comparing Subaru SuprimeCAM of $34' \times 27'$, with which the large scale structure of galaxy distribution at $z > 4$ has been found, the field of view of the current near-infrared cameras would be too small to study the clustering assembly in such large scale.

Further author information: (Send correspondence to T. I.)
T.I.: E-mail: ichikawa@astr.tohoku.ac.jp, Telephone: +81-22-980-6500

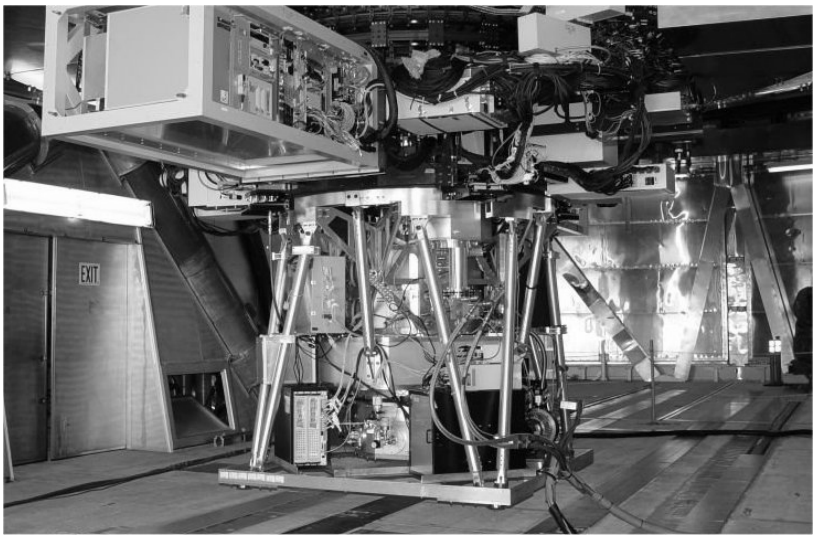

Figure 1. MOIRCS mounted on the Subaru Cassegrain focus.

Since the rest-frame optical emission lines, e.g., Hα, [OI], [OII], etc. for objects at redshift $z > 1$ shift to near-infrared, the spectroscopic observations in the near-infrared give us clues to understanding the nature on the star forming activity and active galactic nuclei of high-z galaxies. Although a lot of time has been devoted to the near-infrared spectroscopy for high-z galaxies, the number of the observed objects is quite limited due to the high background and the low flux in near-infrared. Multi-object spectroscopy, which has been common technology in optical, could be very powerful for the study of the nature of such faint galaxies. However, multi-object spectrographs in near-infrared have not been available as a common instrument for large telescopes.

The superb image quality of Subaru telescope and excellent atmospheric condition at Mauna Kea in Hawaii, especially in near-infrared, enable us to observe fine structures of faint objects. To enjoy the advantages of Subaru telescope and the development of large FPAs in near-infrared, we have constructed Multi-Object InfraRed Camera and Spectrograph (MOIRCS), which is a new facility instrument dedicated for wide-field imaging ($4' \times 7'$) and multi-object spectroscopy in near-infrared (0.8μm-2.5μm). The designing was started in 1999 jointly by Subaru Telescope of National Astronomical Observatory Japan and Institute of Astronomy, Tohoku University. MOIRCS saw the first light in September, 2004. In this paper, we describe the details of the design, performance, and the results of the commissioning observations.

2. OVERVIEW OF MOIRCS

MOIRCS (Fig. 1) has two operation modes of direct imaging and MOS observations. In the imaging mode, MOIRCS provides $4' \times 7'$ field of view with a scale of $0\farcs117$ per pixel using two 2048×2048 HgCdTe (HAWAII2) arrays. The MOS mode allows us to perform multi-object spectroscopy up to 2.5μm with exchangeable cooled slit masks. The schematic structure is depicted in Fig. 2 and the performance is summarized in Table 1.

MOIRCS consists of three main structures, a main cryostat, a MOS mask exchange system, and a support frame. The main cryostat and MOS system have their own mechanical cooler. Motor drivers and controllers, network devices, detector controllers, monitor devices, a vacuum pump for MOS mask dewar and others are mounted on the support structure in a 2 m$\times$2 m $\times$2 m framework. The main dewar houses an optical bench, on which two sets of the identical optics system and HAWAII2 arrays are mounted. The mask dewar is an octagonal shaped vessel attached to the top of the main dewar. The mask storage (referred as "carousel") is enclosed in the MOS mask dewar, which can be shuttered from the main dewar by a gate valve during exchanging the MOS masks. The optical bench is suspended from the inner surface of the main dewar with bracket straps of G10 epoxy glass fiber, which has low thermal conduction and contraction, and keeps stiffness at cryogenic

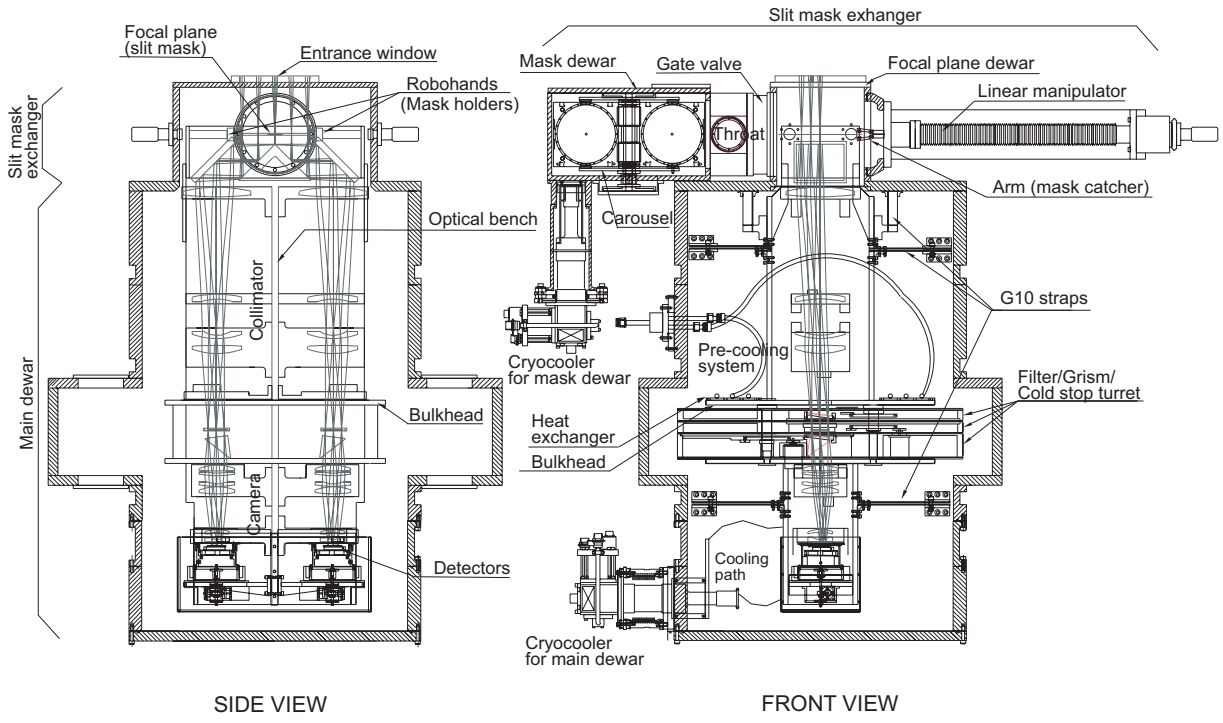

Figure 2. The schematic of MOIRCS.

temperature. The wheels of filters, grisms, and cold stops are located at or near the pupils of the each optics. The weight, including the interface to the Subaru Cassegrain focus, is about 2.3 t in total.

The deflection of the structure from the Cassegrain optical axis should be smaller than 200μm, which is required from the tolerance of the optical system. Since the main and MOS dewars are made of aluminum of low weight, and, in particular, the main dewar is a pile up of many low-cost aluminum tubes, for which junctions are shielded with Viton O-rings, we carefully perform finite element analysis (FEA) for the cryostat structures to determine the appropriate thickness of the cryostat wall and number of support pipes. With respect to the insulation of thermal radiation, because the clearance between the dewar wall and optical bench is very tight, multilayer insulators (MLIs) simply wrap the optical bench as shown in Fig. 3 without hard radiation aluminum shields which are generally applied to infrared instruments. One layer MLI consists of a polyester film of 9μm thickness with thin aluminum coated and a polyester net of 200μm thickness for spacer. Studying the heat flow (thermal conduction via MLI and thermal radiation from the wall of the dewar to the optical bench), we fabricate ten-layer MLIs to minimize the heat transfer.

Since the heat mass in the main dewar is so large that the pre-cooling system with liquid nitrogen (LN_2) shown in Fig. 3 is required for cooling the inner structure in reasonable time. In fact, LN_2 of $\sim$700 liters is consumed for the pre-cooling of the system at the summit of Mauna Kea. The thermal FEA analysis indicates that the cooling-down or warming-up speed of the optical components and detectors should be slower than ~ 5 K h^{-1} to avoid high stress to the components. We also carefully warm the detector with a heater so that the detector temperature always keeps higher than those of other parts to avoid the accumulation of frost on to the detector surface. After the optical bench reaches 100 K, the detectors are kept cooled to 77 K with the speed of $3 \sim 5$ K h^{-1}. After the optical system reaches 77 K at the detectors and 100 K at the optical bench, the mechanical cooler keeps the temperature with the help of MLIs.

The positions of the six filter turrets and the detector mounts are read with low cost hall sensors made of InSb. Although the sensor is not specific for cryogenic use, we confirm that it has positioning accuracy of $\sim 10\mu$m and keeps linearity at 77 K in the range of our practical use ($\pm$1 mm). The detector mount has a linear guide to

Table 1. Performance summary of MOIRCS

Observing modes	imaging, multi object spectroscopy
Field of view	$4' \times 7'$ (imaging), $4' \times 6'$ (spectroscopy)
Wavelength coverage	0.85μm – 2.5μm
Filters	J, H, Ks, K, K_{cont}, H_2, CO, Fe
Detectors	$2 \times 2048 \times 2048$ HgCdTe (HAWAII2)
Pixel scale	$0''.117$
Resolution of point source	FWHM $< 0''.18$
Image quality	Degradation hardly perceptible from center to edge
Background	15.4 (J), 13.4 (H), 14.1 (Ks) mag arcsec^{-2}
Readout noise	31 e$^-$
Grisms	R$\sim$500 (zJ, HK), R$\sim$1300 (JHK) with $0''.5$ slit width
VPH	R$\sim$3000 (in progress)[3]
Total throughputs[†]	0.22 (J), 0.32 (H) 0.31 (Ks) in imaging mode
	0.18 (zJ500), 0.24 (HK500) with grism
Sensitivity	23.8 (J), 22.7 (H), 22.7 (Ks) mag (1 hour, S/N=5, $1''$ aperture)
Slit mask	14 slots for users, 4 slots for common use
Number of slits	$\sim$ 50 slits per sheet
Weight	2.3 t
Size	$2 \times 2 \times 2$m^3

[†] include the telescope

Figure 3. The optical bench dressed with MLI blankets (left) and the LN_2 heat exchanger mounted on the optical bench fringe (right).

adjust the detector position precisely at the camera focus. The focus position of the camera and the tilt of the detector can be checked with the help of the pinhole grid mask set by the MOS exchange system at the Subaru Cassegrain focus. The fine focus adjustment for each detector always keeps high image quality of MOIRCS.

3. OPTICS

Since buttable FPAs like HAWAII2-RG were not available when we started designing MOIRCS in 1999, we decided to divide the Cassegrain field of view. The original idea was to divide the field into four by a pyramid mirror. However, consulting the cost and the difficulties of the optical alignment, we adopted a roof mirror which guides the field of $4' \times 7'$ into two sets of identical optics with each $4' \times 3'.5$ field. Each set of the optics

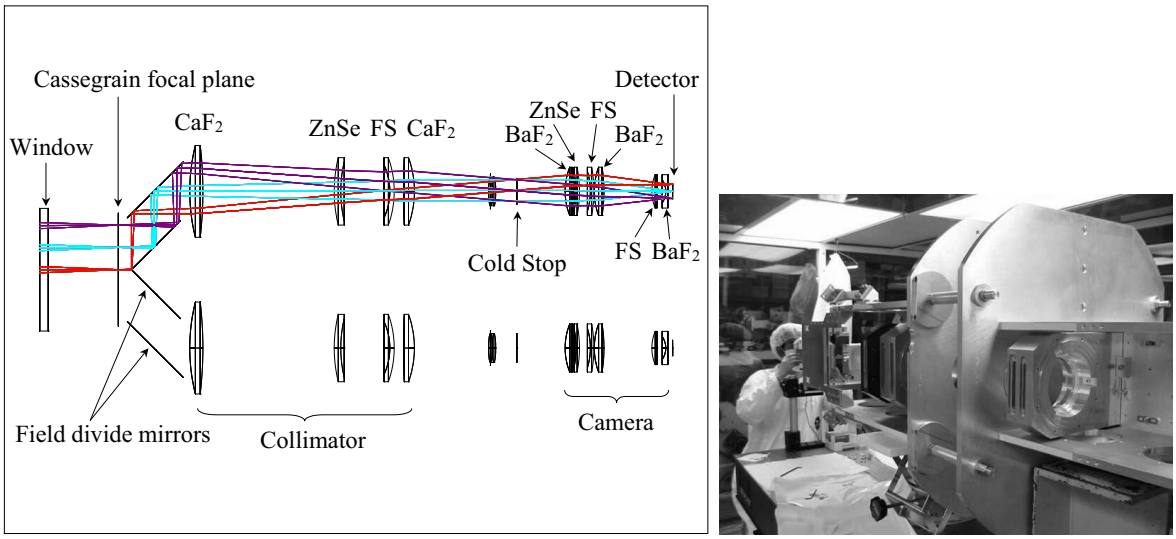

Figure 4. A schematic diagram of MOIRCS optical system (left) and the install on the optical bench.

consists of a four lens collimator and a six lens camera section. The collimator changes light from the telescope to a parallel beam of 50 mm in diameter, where filters with the size of 80 mm $\times$80 mm or ϕ80 mm and grisms are inserted (see Fig. 4). It also makes a sharp image of the telescope secondary mirror so that a cold stop is placed at the pupil image position. The camera re-images the parallel beam on the detectors with a pixel scale of $0\farcs117$. We use CaF_2, BaF_2, ZnSe, and Fused Silica for the lens because of their high transmissions in the near-infrared wavelengths as well as availability of the materials of large size. Gold coated Ultra Low Expansion glass (ULE) is used for the mirrors because the gold has high reflectivity in the near-infrared and is chemically stable, while the ULE has a small thermal expansion coefficient. We use CaF_2 for the main dewar window because of its high transmission over the longer infrared wavelength and because good heat conductivity prevents frost from its outer surface. The designed optics shows good performance. The ensquared energy within 2-pixel square exceeds 85 % in the wavelength range over the whole field of view with no practical chromatic aberrations. We find from the analyses that the designed performance is kept with the reasonable tolerances in terms of fabrication and optical alignment. We made the opt-mechanical parts including lens mounts and an optical bench of aluminum (Al6061-T651), because of the following reasons; Al6061-T651 has good machinability and high thermal conductivity. It is heat-treated, and the nature of thermal shrinkage is well known. Simple plate springs made of phosphor bronze are used to hold the lenses and mirrors precisely under both the room and cooled temperature. The details of the optical design, performance of the designed optics, and the tolerance analyses are described in Ref.[4]

The lens mounts are heat-treated again before the final machining to reduce stress possibly caused by the rough machining. We measure all the cardinal dimensions of the lens mounts using a high precision 3D measuring device and then we re-design the optics, by adjusting the intervals of the lens mounts, or trading the lenses between two channels, with the dimensional data of the lens mounts we measure and the data sheets of the lenses and mirrors supplied by the manufacturer.

The opt-mechanical parts are assembled in the laboratory at Subaru Telescope. We use an alignment telescope and an alignment target to precisely locate the opt-mechanical parts (see Fig. 4). First, the optical bench is precisely flattened using its reinforcement structures, because the optical bench itself is bent by gravity. We measure the flatness of the optical bench by putting a lens mount with the alignment target at several points along the optical path on the optical bench, and fixed the flexure if needed. We flip the optical bench and follow the same procedure for the other side of the optical bench, because two optical channels are placed back to back at each side of the optical bench. The lens mounts are, then, put on the optical bench using locating blocks. We use stainless shims to adjust the decenter and tilt if necessary. Eventually, however, we end up using only a few

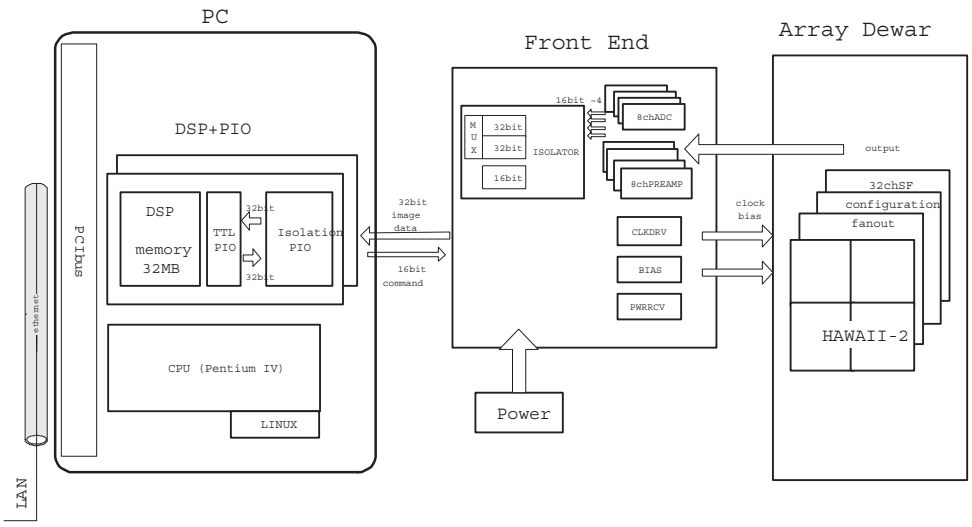

Figure 5. A schematic diagram of TUFPAC.

shims because the lens mounts and optical bench are precisely fabricated. The filters are tilted (~ 6 degree) so that the light coming from the center of the Cassegrain focal plane enters perpendicularly into the filter.

We design the grisms of spectral resolutions of R=500 (hybrid) and 1300 (ruled) with 0.″5 slit with. MOIRCS equips two kinds of R500 grisms, which we call zJ500 and HK500. Both R500 grisms use 1st diffraction order to cover z to J bands and H to Ks band, respectively, while JHK1300 grism covers J, H, and Ks bands with diffraction orders of 4th, 3rd, and 2nd, respectively. We use Fused Silica and regular resin as a prism and diffraction grating material for the hybrid grism, and KRS-5 for the directly ruled grism. For the spectroscopy with higher resolution, we are now fabricating VPH disperser with R=3000.[3]

The cold stop is an important component in infrared instruments to reduce thermal background radiation. Therefore, the position of the cold stop relative to the image of the telescope secondary mirror should be carefully aligned. The acceptable tolerance for the position of the cold stop is estimated to be 0.5 mm. To see the decenter of the cold stop when MOIRCS is operated with Subaru telescope, we design an additional optics called "pupil viewer". The pupil viewer consists of four small BK7 lenses installed in the turret which is located between the cold stop and the first camera lens. When the pupil viewer is inserted in the optical path, it focuses the images of the cold stop and the telescope secondary mirror on the detector with the help of the camera optics. Because the resolution of the pupil viewer is $\sim 5\mu$m, we can observe the position of the cold stop with enough accuracy to adjust the cold stop to the proper position.

4. DETECTOR CONTROL SYSTEM

Fast and efficient acquisition of FPA data with low noise performance is one of fundamental goals to be achieved for astronomical instruments. In addition, the cost performance and easy maintenance are also important aspects, so that array control systems have often been designed for a specific FPA to make the system as simple as possible. In this context, we made a low cost array control system TUFPAC (Tohoku University Focal Plane Array Controller),[5] which is an array control system originally designed for flexible control of HAWAII2 array and fast and efficient acquisition of the image data. It is applicable to FPAs in optical with minor changes of front-end electronics. Figure 5 shows the schematic configuration of TUFPAC.

TUFPAC consists of a Linux personal computer (PC) equipped on the PCI bus with a commercially available digital signal processor (DSP) board, front end electronics wired to HAWAII2 FPA, and linear power supplies. Linux is not capable of real-time control, which is requisite for the operation of FPAs. Real time OS is usually expensive, while DOS system is outdated. Another promising method is the system based on DSP technology.

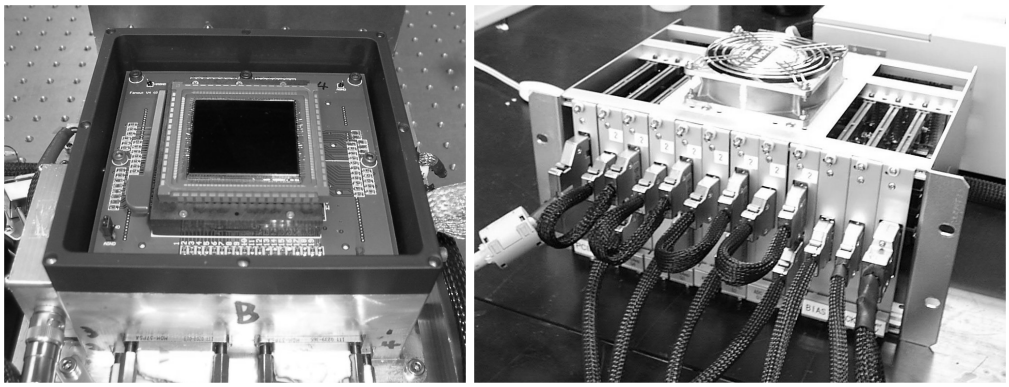

Figure 6. The detector on the mount (left) and the front end electronics (right).

DSP, which is one of the simple methods to realize the real-time operation of FPAs, is capable of sending clock signals independently from PC and receiving the detector data following the operation code stored in the memory of DSP. We use a commercially available DSP board, which equips one DSP of 1 GFLOPS and 32 MB RAM memory. Since the data size of one frame from HAWAII2 is 16 MB, 32 MB is large enough to store the image data. Another 16 MB can be used for working area if necessary. The speed of 1 GFLOPS is fast enough for arithmetic calculation or data processing of image in the frame memory. The device driver of the DSP board for Linux is available from the vendor. The DSP programs are written in C language and compiled to DSP code. An optional parallel board of 32-bit inputs and 32-bit outputs is available for the DSP board (TTL PIO in Fig. 5). Since the parallel board is based on TTL logic, we designed the isolation board, which isolates the PIO from the front-end electronics with photo couplers (Isolation PIO in Fig. 5). The isolation board is used on the PCI bus, where the PCI bus supplies 5 V DC. (The board is not based on PCI protocol). We use 16-bit outputs from 32 outputs of TTL PIO for the operation of HAWAII2 array. The input port of 32 bits is fully used to receive the digital data simultaneously from two ADCs. To receive all data from a HAWAII2 array, the operation is repeated twice and 16 times for 4- and 32-output modes, respectively.

The front-end electronics consists of a power-receiving board (PWRRCV), an isolation board (Isolator), bias board (BIAS), clock driver board (CLKDRV), four 8-channel pre-amplifier boards (8chPREAMP), and four 8-channel analog-to-digital converter boards (8chADCs). The electric parts of surface mount types are used to make the system as compact as possible. All circuits are wired on VME-3U size cards (Fig. 6). The backplane board has 96 buses, out of which 64 buses are used for the digital outputs of four ADCs. Another 32 buses are allocated to the clock signals, control signals, and power supplies. The PGA pins of the ceramic package not wired to HAWAII2 array are used for the heat sink. A copper plate, on which socket pins are adhered, is inserted to the ZIF socket from the backside. Two small Pt resistors of a surface mount type with size of 3.2 mm $\times$ 1.6 mm are directly soldered to the ZIF pins for the monitor of the detector temperature. First, the operation code is transferred from PC to DSP. The PC operated by Linux OS sends the clock patters to DSP. Triggered by PC, DSP sends clock signals to each front-end electronics by way of Isolation PIO. Then the clock signals are transferred to HAWAII2. The analog data coming out from the output ports of the detector and converted to digital data in the front-end electronics. Then the PC receives the frame data and stores them in a hard disk in FITS format. One DSP board is responsible for the operation of one set of front-end electronics.

The data acquisition and control by TUFPAC shows good performance for the operation of the HAWAII2 array. The readout noise in CDS is $31e^-$ when MOIRCS is mounted at the Cassegrain focus of Subaru telescope. Since the laboratory test gives $\sim 17e^-$, the control or network devices on MOIRCS possibly generate the systematic noise. In fact, the multisampling with 16 readouts gives the nose as high as $15e^-$. It does not obey statistic law that the random noise decreases with $1/\sqrt{N}$ (N is the number of sampling). We use 32ch off-chip source follower amps with FET pairs (32chSF in Fig. 5) to avoid the glow of HAWAII2. The glow is negligible, compared with sky background, for the imaging observation with wide band filters, while it should be depressed for observations with narrow band filters or spectroscopic observations with low background. Therefore, the

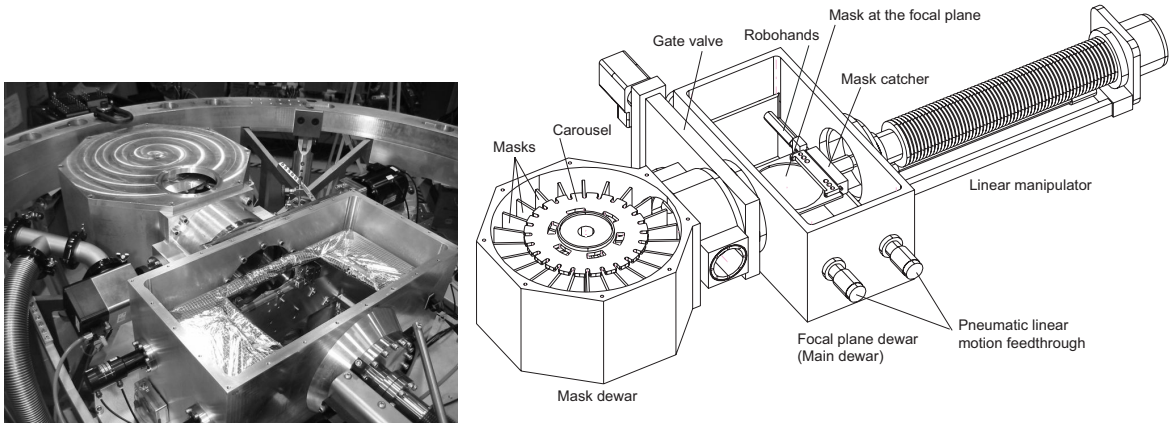

Figure 7. The slit mask exchanger.

current source for the cell is supplied via external 200 kΩ resistors, instead of supplying the current to the gate power and gate bias (BIASPOWER=0, BIASGATE=0). Although the internal glow is hardly perceptible with this configuration, we find the serious cross talk in the octants of each quadrant of HAWAII2 if the 32-out mode is selected, while no cross talk is seen for the 4-out mode. Therefore, we have adopted the 4 mode. Because of a large format of HAWAII2, it takes about 10 seconds to read all pixels in the 4 mode, while near-infrared standard stars are generally too bright for 8-m class telescopes with such long exposure time. Therefore, short exposures for bright stars are performed with a partial readout method; the small region around standard stars are read and stored. We operate the partial read with the shortest exposure time of 1 s.

5. SLIT MASK EXCHANGER

One of the difficult issues in multi-slit spectroscopy in K band is how to take care of a cooled mask which should be fixed properly at the focal position and exchanged by observer's demand. It would be best if the slit mask set prepared by observes could be changed in reasonable time without warm up the main dewar. The schematic of the novel mask exchanger of MOIRCS is shown in Fig. 7. Since the details are described by Ref.[6] in this volume, we give here a thumbnail sketch of the mechanics.

The mask exchanger consists of a carousel, which holds 19 slit mask sheets, an arm with a mask catcher, and four robohands. A gate valve shutters the dewar during the mask exchange. The mask should be cooled below 150 K to reduce the thermal radiation from the mask surface. Aluminum sheets are used for slit mask because aluminum has high thermal conductivity and good machinability. We examine the thermal contraction factor with the image of pinhole or slit masks and find that it is constant and uniform ($\pm 0.02\%$) at ~ 100 K over the sheet regardless of different patterns of pinhole or slit positions. The size of the slit mask is 180 mm in diameter and 0.075 mm in thickness. Slits are made by a laser cutter with the speed of about 10 m per slit of typical size (1 mm $\times$ 0.1 mm). More than 50 slits can be placed on a slit mask at once. The masks are suspended at the carousel by magnets in the mask dewar, so that they are cooled efficiently through the heat sink attached to the carousel and held safely during observations. The time for the cooling down and warming up of the mask dewar should be so short that masks are replaced during daytime. Therefore we use a cryo-cooler for specific purpose of cooling the MOS mask dewar to shorten the cooling time. Nevertheless we need 2 days to replace the slit set at this moment. Rotating the carousel, we select one of the slots. The mask catcher with a linear manipulator in vacuum environment picks a mask up and carries it from the carousel to the main dewar. Then the robohands steadily grip the mask on the focal plane during observations. The catcher and gripper are operated pneumatically. The mask exchange takes about 4 minutes.

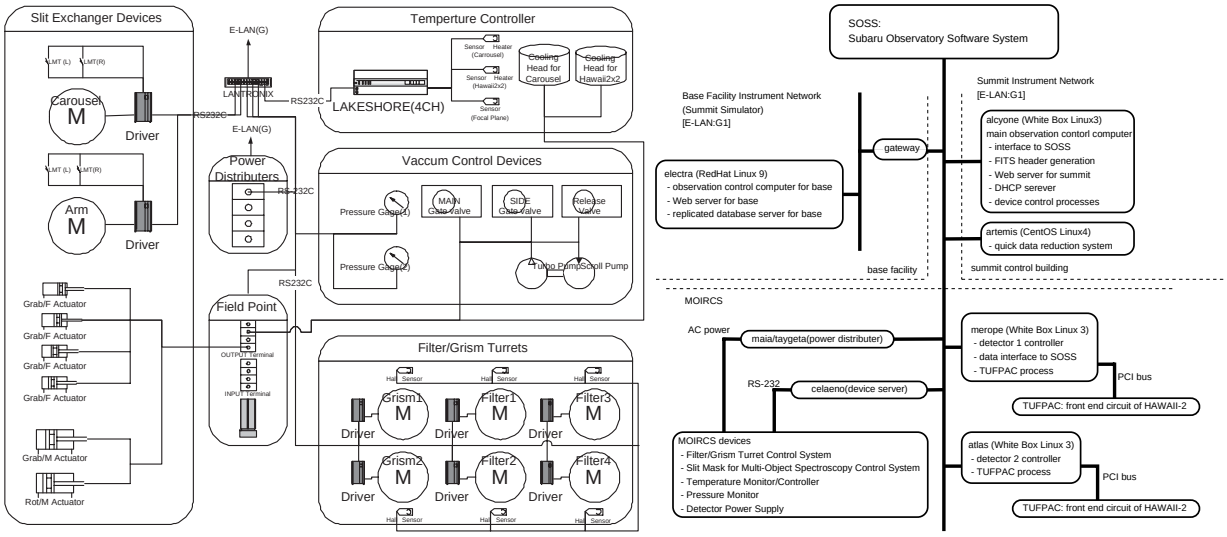

Figure 8. MOIRCS hardware configuration (left) and the allocation block diagram of the network distributed system (right).

6. HOUSE KEEPING AND CONTROL SOFTWARE SYSTEM

House keeping system consists of motor drivers, air suppliers, temperature monitors, vacuum monitors, data handling electronics for various sensors, and power supplies for all these devices. The schematic is shown in Fig. 8. The house keeping is controlled by the software system, T-LECS (Tohoku University – Layered Electronic Control System), which is a PC-Linux based network distributed system.[7] The system hardware consists mainly of three Linux personal computers (PCs) and the control devices distributed on a TCP/IP network. Two PCs are used for the readout of each HAWAII2 data, respectively, and another PC is allocated to the user interface and database server. T-LECS has the device control interface and two user interfaces. One of the user interfaces communicates with the Subaru Observation Software System (SOSS). Another provides us tools for the direct access to the MOIRCS devices. There are a large number of configuration parameters (~ 150 data) and status data (~ 120) to perform the observation with MOIRCS and Subaru telescope. Sometimes new data should be added or some deleted in the course of the progress of MOIRCS construction. Therefore the interface should be flexible in terms of the system integration and modification. Then we employ an SQL database system to assist the communication with each other.[8] Similar approach is seen in previous studies, e.g., Ref.,[9] which produce source codes, documents, GUI applications from relational database. Thanks to the progress of open source softwares and PC architecture, we can construct the control system dealing real time data processing on PC/Linux based operating system.

To help the communication among the device and user interfaces, we define three layers in T-LECS; they are an external layer for user applications, an internal layer for device applications, and a communication layer. The database server for the communication layer stores most of the system data, for example, configuration information of the removable components, the status of devices, and information to generate FITS headers. The most important function of the communication layer is to convert the names of removable components from "external name" to "internal name" and vice versa. In the external layer, applications use external names, which abstract the components of MOIRCS seen from the outside world. Then the applications in the communication layer, referring the configuration information in the database, translate these external names to internal names, which are comprehensible to the applications controlling the devices. Consequently, the applications in the internal layer use the internal name.

Most of the devices controlled via RS232C interface are accessible from TCP/IP network using a TCP/IP to RS232C converters. Some are controlled from PCs via the PCI bus, network interface, and serial ports. These network distributed hardwares make the system development very flexible. To enjoy the flexibility, we

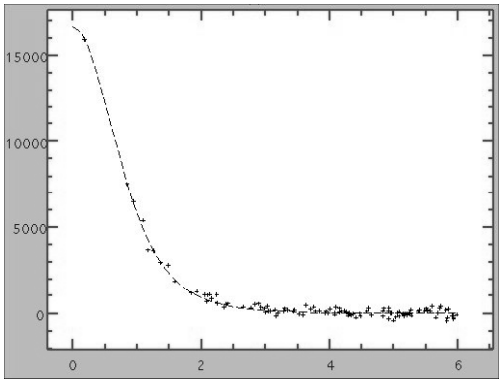

Figure 9. The sharpest PSF found. The abscissa indicates radius from a center of profile in pixel. FWHM = 1.5 pixels correspond to 0.″176.

apply TCP/IP as the interprocess communication. The SQL database server is also accessible from network. This communication method makes it easier to distribute the T-LECS processes. Therefore we can locate the processes according to the load to the system and hardware connections of the PCs. We design the T-LECS library with an object oriented scheme, which boosts the flexibility of the application structure to our library. When we need a new application using T-LECS, we can code it using the library. We describe the system schema in UML. Therefore, it is easy to convert the system to those with different programming languages in the same scheme. In fact, we have ported T-LECS library to PHP to develop web applications.

We have successfully performed the commissioning observation with T-LECS and enjoyed the flexibility of the system through the system configuration information sent from the layered structure, the hardwares and the allocation of the applications from the network distributed system, and the application structure from the object oriented design.

7. EVALUATION OF THE PERFORMANCE WITH SUBARU TELESCOPE

After the verification test with the simulator in the laboratory, we conducted the evaluation of MOIRCS performance in the commissioning observation from Sep. 2004 (first light) to Feb. 2006 both for the imaging and MOS spectroscope mode.

7.1. Imaging Observations

The relation between the detector plane and the Cassegrain focal plane of the telescope is evaluated by taking a star field, where properly bright stars are sparsely distributed over the field of view, under the good seeing condition at various telescope focus positions. We pick up only the bright stars with good signal to noise ratio (S/N) and calculate FWHM of their flux profiles. We see that FWHMs are nearly uniform ($\sim$ 2.6 pixels) over the field of view and the peak-to-peak variation is less than 1 pixel. Figure 10 shows the flux profile of the stellar object with the smallest FWHM we have found. Its FWHM is 1.5 pix, which correspond to 0.″176. Although we do not know whether the best image obtained is limited by seeing or optics, the result is satisfactory enough for usual imaging observations. As a conclusion, we note that the image degradation may be a subject only at the best seeing.

We evaluate the lateral chromatic aberration by comparing the positions of the stellar objects taken sequentially with the different filters. The maximum difference of the magnification is 0.017 % between J and Ks band which corresponds to 0.25 pixel or 30 mas at the edge of the detector. Because the maximum difference of 30 mas or 0.017 % is small enough, we conclude that MOIRCS has no lateral chromatic aberration practically. The axial chromatic aberration is evaluated by putting a grid pinhole mask on the Cassegrain focal plane and seeking the best focus position using through focus technique for each filter. Comparing with the focal depth of the optics ($\pm$150μm), the best image quality, which is almost the same, among the different filters can be obtained

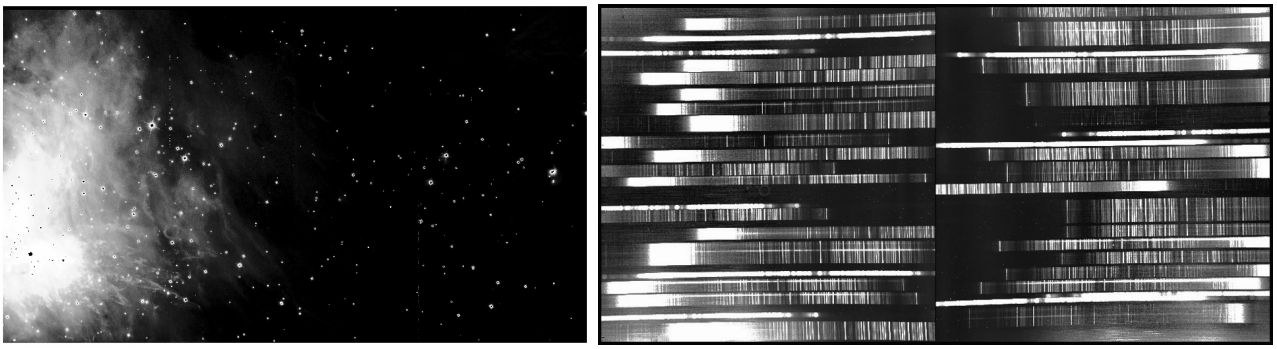

Figure 10. A Ks band image (left) and the multi object spectra with R500 HK grism (left) in Orion region

without adjusting focal position for each filter. In other words, MOIRCS has no axial chromatic aberration. It is also very important to see whether the distortion correction function depends on the telescope position. We investigate the effect by taking the image of the grid pinhole mask at various telescope positions. We apply the distortion correction function obtained at zenith position to the images taken at the other telescope positions, and compared the coordinates of the pinholes. The dependence on the telescope position is less than 0.1 pix and is negligible compared to the intrinsic error of 0.3 pix.

We observed the stars listed in the United Kingdom Infrared Telescope (UKIRT) standard star catalog with J, H, and Ks band. The observed throughputs (e.g., 0.32 in H band) are smaller than expected in all the photometric bands. The maximum difference is $\sim$ 21 % in H band. We note that there are some uncertainties in deriving the expected throughput such as atmospheric extinction, the reflectivity of the telescope, the transmission of the antireflection coatings, the gain of the electronics, and the detector quantum efficiency. The calculated throughputs might also be affected by uncertainty because of the small number of observing points. Among these uncertainties, we especially suspect that the transmission of the antireflection coating might be degraded because the molecules stick onto the coating. The molecules could be the outgas released from the inner components of the cryostat and stick on the coating when the optics are cooled. They possibly make frost in the worst case.

The background brightness is obtained with the standard stars and compared with the average of Mauna Kea and those of CISCO and ISSAC. Although there is only small number of observations available yet, the value agrees fairly well in J and H band, while it is 0.4 $\sim$ 1.2 magnitude fainter in Ks band. The higher background for CISCO and ISSAC could be due to the thermal radiation from a tertiary mirror because they are located on Nesmith focus.

We have observed a strong tilt of the detector bias (sometimes called as "reset anomaly" or "bias tilt") in some engineering detectors. The anomaly is greatly depressed with the method by sending pixel clock with the same pixel rate of reading soon after resetting frame and before finishing exposure. Since the method increases the overhead time and, as the consequence, makes the readout time (or shortest exposure time) longer and the science grade detectors of MOIRCS shows no serious anomaly, we do not apply the method.

7.2. MOS Observations

As to the MOS observation, even small positional offset of targets and slits would not give us high S/N spectra. The setup of targets on the slit mask in reasonably short time is also important in terms of saving time. Since the detail results of the performance for the spectroscopic observations are given in this volume,[6] we present here the summary of the results. First, we point the telescope to a target field, and then take the image of the field without a slit mask. Next, we set a mask at the focal position and take an image of the mask. The positions of alignment stars and the guide holes are measured on the images. Using the difference data, the telescope is pointed again to the proper position as to center the stars at the holes. The iteration is repeated three to four times, which depends on the brightness of the alignment stars. It takes about 30 min on average, as of writing this paper, to center the stars within an offset of 0.″1, reasonably smaller than the typical slit width 0.″5.

The spectral resolution and dispersion of the grisms are measured with a long-slit spectroscopic observation of night sky emission lines with 0.″3 slits and found to agree with the original specifications within errors. The spectroscopic efficiency is also obtained with A-type star with known magnitude as shown in Table 1.

Random differences of target and slit positions would also give us inhomogeneous spectra. The targets should not be slipped off slits. The random error comes from various reasons, e.g., non-uniformity of the thermal contraction of the aluminum mask, the uncertainty of the distortion correction for the mask-design image, the position error of a laser cutter. To study the random error, we observed several regions, e.g., globular clusters, star clusters, and galaxy fields. The rms residuals of the target position from the slit center are about 0.″03 – 0.″04, which is small enough again, compared with the typical slit with of 0.″5. Note that the residual does not depend on the number of slits and holes and therefore that the number of slits does not affect the uniformity of the thermal contraction of the aluminum sheet. In long exposures, the telescope, mask, and FPAs are decenter due to the flexure of the instrument. Target objects could be lost from the slit during long observations. In fact, we saw the effect in the commissioning observations. However, since the decenter is the same for targets over the slit mask, small telescope offset returns the targets to the slit center. The proper guiding will allow us long exposure observations.

Although there is no sign of stray light in imaging mode, thanks to the careful design of the optical tubes covering the optics and detectors, as proved by the result of the low background in Ks band, we find the strong thermal stray light in spectroscopic mode from the entrance holes for the mask exchange. We are now designing the structure to cover the holes.

ACKNOWLEDGMENTS

We would like to thank the Director, all members of Subaru telescope, and Shuji Sato for their continuous support and encouragement. The machine shop of Tohoku University fabricated the detector mounts and others. We owe Masayuki Akiyama the evaluation of spectroscopic performance. Daigo Matsumoto, Kenshi Yanagisawa and Ken'ichiro Asai contributed to the development of the detector controller in the early stage. This research was supported by grant-in-aid from scientific research of the Ministry of Education, Culture, Sports, Science and Technology (09440088, 11554005, and 14300059).

REFERENCES

1. A. Moorwood *et al.*, "ISSAC sees first light at the VLT," *The Messenger* **94**, pp. 7–9, 1998.
2. K. Motohara *et al.*, "CISCO: Cooled Infrared Spectrograph and Camera for OHS on the Subaru Telescope," *PASJ* **54**, pp. 315–325, 2002.
3. K. Ichiyama, T. Ichikawa, N. Ebizuka, R. Suzuki, *et al.* 2006 (in preparation).
4. R. Suzuki, C. Tokoku, T. Ichikawa, and T. Nishimura, "Optical design of MOIRCS," *SPIE* **4841**, pp. 307–318, 2002.
5. T. Ichikawa *et al.*, "Tohoku University Focal Plane Array Controller (TUFPAC)," *SPIE* **4841**, pp. 376–382, 2002.
6. C. Tokoku *et al.*, "Infared multi-object spectrograph of MOIRCS," *SPIE* **6269**, 2006 (in this volume).
7. T. Yoshikawa *et al.*, "T-LECS: The Control Software System for MOIRCS," in *Astronomical Data Analysis Software and Systems XV*, C. Gabriel, C. Arviset, D. Ponz, and E. Solano, eds., *ASP Conference Series,*, 2006 (in press).
8. T. Yoshikawa *et al.*, "Application of SQL database to the control system of MOIRCS," *SPIE* **6274**, 2006 (in press).
9. D. Clarke and S. Allen, "Using a Data-Driven Model for Instrument Software Development," in *Astronomical Data Analysis Software and Systems IX*, N. Manset, C. Veillet, and D. Crabtree, eds., *ASP Conference Series* **216**, pp. 16–20, 2000.